Neoplasia 62 (2025) 101139

Contents lists available at ScienceDirect

Neoplasia

journal homepage: www.elsevier.com/locate/neo

Original Research

Combining the RCAS/tv-a retrovirus and CRISPR/Cas9 gene editing systems to generate primary mouse models of diffuse midline glioma

Sophie R. Wu [a], Julianne Sharpe [b], Joshua Tolliver [a], Abigail J. Groth [a], Reid Chen [a], María E. Guerra García [c], Vennesa Valentine [d], Nerissa T. Williams [a], Sheeba Jacob [a,e], Zachary J. Reitman [a,e,f,g,*]

[a] Department of Radiation Oncology, Duke University, Durham, NC 27710, United States
[b] Department of Biology, College of Arts and Sciences, University of Kentucky, Lexington, KY 40506, United States
[c] Department of Biomedical Engineering, Washington University, St. Louis, MO 63130, United States
[d] Department of Pharmacology, Duke University, Durham, NC 27710, United States
[e] The Preston Robert Tisch Brain Tumor Center Duke University Medical Center, Durham, NC 27710, USA
[f] Department of Pathology, Duke University Medical Center, Durham, NC 27710, USA
[g] Department of Neurosurgery, Duke University Medical Center, Durham, NC 27710, USA

ARTICLE INFO

Keywords:
Diffuse midline glioma
Midline glioma
CRISPR
Retrovirus
Genetic mouse model
Cre/loxP

ABSTRACT

Diffuse midline gliomas (DMGs) are lethal brain tumors that arise in children and young adults, resulting in a median survival of less than two years. Genetically engineered mouse models (GEMMs) are critical to studying tumorigenesis and tumor-immune interactions, which may inform new treatment approaches. However, current midline glioma GEMM approaches are limited in their ability to multiplex perturbations and/or target specific cell lineages in the brain for genetic manipulation. Here, we combined the RCAS/tv-a avian retrovirus system and CRISPR/Cas9 genetic engineering to drive midline glioma formation in mice. CRISPR/Cas9-based disruption of *Trp53*, a tumor suppressor that is frequently disrupted in midline gliomas, along with the oncogene PDGF-B resulted in high grade tumor formation with moderate latency (median time to tumor formation of 12 weeks). We confirmed CRISPR-mediated *Trp53* disruption using next-generation sequencing (NGS) and immunohistochemistry (IHC). Next, we disrupted multiple midline glioma tumor suppressor genes (*Trp53, Pten, Atm, Cdkn2a*) in individual mouse brains. These mini-pooled *in vivo* experiments generated primary midline gliomas with decreased tumor latency (median time to tumor formation of 3.6 weeks, $P < 0.0001$, log-rank test compared to single-plex gRNA). Quantification of gRNA barcodes and CRISPR editing events revealed that all tumors contained cells with various disruptions of all target genes and suggested a multiclonal origin for the tumors as well as stronger selection for *Trp53* disruption compared to disruption of the other genes. This mouse modeling approach will streamline midline glioma research and enable complex experiments to understand tumor evolution and therapeutics.

Introduction

Diffuse midline gliomas (DMGs) are tumors that arise in midline brain structures such as the brainstem or thalamus and histologically resemble glia, the supporting cells of the brain. DMGs are highly aggressive tumors of children and young adults, which result in a median survival of less than two years following diagnosis [1]. Due to their localization to essential midline brain structures and diffuse nature, complete surgical resection is not possible, leaving radiation therapy as a standard treatment to temporarily palliate the tumors. While radiation therapy is capable of halting progression and minimizing symptoms, tumors inevitably progress, making DMG incurable

Abbreviations: DMG, diffuse midline glioma; GEMM, genetically engineered mouse model; RCAS/tv-a, replication-competent avian leukosis virus splice-acceptor/tumor virus A; CRISPR, cluster regularly interspaced short palindromic repeats; NGS, next-generation sequencing; IHC, immunohistochemistry; PDGF-B, platelet-derived growth factor B; BFP, blue fluorescent protein; gRNA, guide RNA; PCR, polymerase chain reaction; NNC, Nestin-tv-a; Nestin-Cre, Rosa26-loxP-Stop-loxP-Cas9-EGFP; FFPE, formalin-fixed paraffin-embedded.

* Corresponding author at: Department of Radiation Oncology, Duke University Medical Center, Durham, NC 27110, USA.
E-mail address: zjr@duke.edu (Z.J. Reitman).

https://doi.org/10.1016/j.neo.2025.101139
Received 11 December 2024; Accepted 10 February 2025

[2,3]. Preclinical models such as genetically engineered mouse models (GEMMs) are key to the study of cancer mutations and their role in tumor development, making them crucial for the development of novel effective treatments for DMGs.

RCAS/tv-a is a retroviral delivery system that can deploy genes of interest to specific cell lineages, allowing for precise tumor modeling in organs of interest [4]. For instance, to model brain cancer arising from neural stem cells, Nestin-positive neural stem cells can be engineered with a cell surface receptor for avian retrovirus ALV, subgroup A (tv-a). Replication-competent avian leukosis virus splice-acceptor (RCAS) retrovirus vectors, secreted by injected avian fibroblast cells, target cells with the tv-a receptor, activating oncogenes and inactivating tumor suppressors to promote tumorigenesis. This system has been used to model a variety of brain tumors such as adult gliomas [4,5], medulloblastomas [6,7], and brainstem gliomas including DMG [8,9].

Beyond its precise modeling capabilities, the RCAS/tv-a system offers several advantages for scientific research in oncology. Mice are fully immune competent, allowing for a more accurate study of tumor-immune interactions that are critical to developing new immunotherapies [10–12]. Additionally, these autochthonous models allow the study of the process of tumorigenesis that cannot be observed in transplant-based tumor models such as xenografts or allografts [13]. When combined with genetic engineering, researchers can more thoroughly probe the effects of gene expression knockdown and how that may impact tumorigenesis. However, the current model of mouse breeding to generate mice with desired combinations of genetic alterations in their germline is cumbersome, requiring months to years to generate mice with multiple genetic perturbations to examine complex molecular interactions.

To address these challenges, we sought to establish a more efficient approach to rapidly perturb multiple genes of interest when generating primary midline gliomas in mouse models. Cluster regularly interspaced short palindromic repeats (CRISPR)/Cas9 has emerged as a precise genome editing technology, making it a powerful tool in cancer modeling. The system's ability to remove, edit, or add sections of DNA has been leveraged in a variety of preclinical mouse models, ranging from *in vivo* somatic gene editing to *ex vivo* targeting of cellular transplant models and more [14–17]. Recently, Oldrini *et al.* characterized an approach to combine the RCAS/tv-a mouse modeling system with CRISPR/Cas9 gene editing technology to generate supratentorial adult gliomas in mice [18]. However, to our knowledge it has not been examined whether RCAS/tv-a can be combined with CRISPR/Cas9 to model pediatric and/or midline-based gliomas such as DMG. Further, it has not been demonstrated whether multiple (>3) CRISPR/Cas9 perturbations can be introduced to the same primary mouse glioma.

Here we describe a mouse model for DMG by combining RCAS/tv-a and CRISPR/Cas9 to induce gliomas in the mouse midline. We found that the combined RCAS/tv-a and CRISPR/Cas9 technology could drive midline gliomagenesis to model DMGs in a flexible lineage- and spatially-controlled manner. We demonstrate that Cre-recombinase, a key component of the system, can be delivered either via retroviral delivery or via expression from a lineage-restricted promoter in the mouse germline to drive tumor formation. We executed a pooled *in vivo* experiment by simultaneously delivering guide RNAs (gRNAs) targeting multiple tumor suppressor genes relevant to DMG and noted decreased tumor latency. Disruption of all targeted genes was represented in the tumors, which could be quantified using next-generation sequencing (NGS) approaches. These results describe a flexible primary mouse model of DMG that may be useful for future research probing the effects of specific genetic perturbations on tumorigenesis, tumor evolution, and treatment response.

Materials and methods

Mouse strains

Expression of Cas9 in neural stem cells was achieved by cross-breeding existing mice with mice containing Rosa26-lox-Stop-lox-Cas9-EGFP (Jackson Laboratory Strain #024857) [19], Nestin-Cre (Jackson Laboratory Strain #003881) [20], and Nestin-tv-a (Jackson Laboratory Strain #003529) alleles [21]. While Rosa26-lox-Stop-Cas9-EGFP and Nestin-tv-a were homozygosed, Nestin-Cre was maintained in a heterozygous state.

gRNAs targeting DMG relevant genes

The Broad Institute's CRISPick tool [22] or previously reported gRNAs [18] were used to identify gRNAs to disrupt DMG-related genes within the mouse genome: *Atm, Cdkn2a, Pten, Trp53* (Supplementary Table 1). The results were analyzed for efficiency using the Harvard Medical School's Drosophila RNAi Screening Center (DRSC)/Transgenic RNAi Project (TRiP) CRISPR Efficiency Prediction tool. Sequences with higher efficiency scores were selected for eventual cloning into RCAS vectors.

Plasmid cloning to generate RCAS vectors

RCAS-gRNAs vectors targeting DMG genes of interest were generated, including *Trp53, Atm, Cdkn2a, Pten,* and a nontargeting control (Cntl). BbsI restriction digestion and ligation were used to clone each 20-bp gRNA spacer (Supplementary Table 1) into each of two separate pDONR entry vector plasmids (Addgene Plasmid #136405, #136409). Each pDONR plasmids contain the following components: (i) U6 promoter, (ii) gRNA scaffold, (iii) gRNA insertion site, (iv) PGK promoter, (v) platelet-derived growth factor B (PDGF-B) or blue fluorescent protein (BFP), and (vi) flanking AttL sites for Gateway Cloning (RCAS-gRNA-BFP and RCAS-gRNA-PDGFB, respectively). Gateway LR Clonase II (ThermoFisher #11791020) was used to shuttle the gRNA-containing inserts into the destination vector RCASBP-Y DV, which contains retroviral machinery (Addgene Plasmid #11478). *E. Coli* was transformed with these plasmids, and resulting colonies were miniprepped to isolate plasmids. Whole plasmid sequencing (Plasmidsaurus) was used to confirm accurate construction.

Cell culture

DF1 chicken fibroblast cells are cultured in media containing Dulbecco's Modified Eagle Medium (DMEM) (ThermoFisher #30-2002), 10 % Fetal Bovine serum (ThermoFisher #A5670701), 100 U/mL Penicillin (ThermoFisher #15140122), 100 μg/mL Streptomycin (ThermoFisher #15140122), 2 mM l-Glutamine (ThermoFisher #25030081), and 250 μg/mL Amphotericin B (ThermoFisher #15290026) as described previously [23]. 30 % confluent DF1 chicken fibroblast cells were transfected with RCAS plasmids using X-tremeGENE^{TM} 9 DNA Transfection Reagent according to the manufacturer's instructions (Sigma Aldrich #6365779001). Cells were confirmed for appropriate expression by transfecting a set of DF1 cells with the RCAS-GFP plasmid and confirming fluorescence on the microscope 48 h after the procedure's completion. Virus-secreting cells were harvested for midline injection as described [23]; when harvesting DF1 cells from different pools of cells each transfected with different plasmids, cells from all flasks are added together in a 1:1 ratio.

Intracranial injections with harvested DF1 cells

Mice post-natal day 3-5 were intracranially injected with 1 μL containing 100,000 DF1 cells using a Hamilton syringe, inserting the needle about 2 mm below the skin of the pup's head between the ears in the

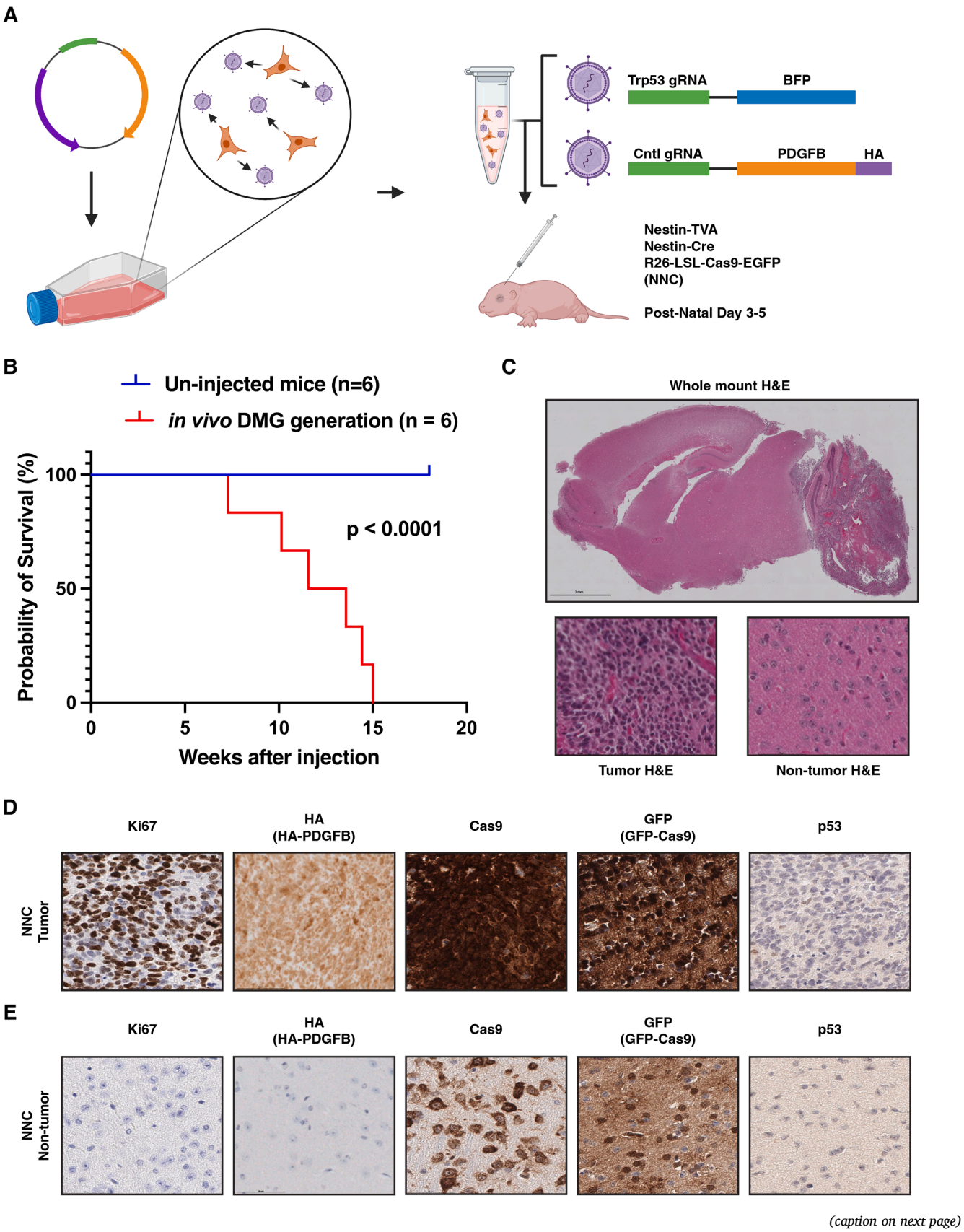

(caption on next page)

Fig. 1. Generation of primary DMGs in mice using CRISPR/Cas9.
(A) Post-natal day 3-5 NNC mice were intracranially injected with virus-secreting DF1 chicken fibroblast cells transfected with RCAS-Trp53-gRNA-BFP and RCAS-Cntl-gRNA-PDGFB plasmids.
(B) Kaplan-Meier survival analysis of mice that received and did not receive intracranial injections of virus-secreting fibroblast cells on post-natal day 3-5. P-value for log-rank test comparison between groups.
(C) Whole mount (top) and H&E slides showing tumor (bottom left) and non-tumor (bottom right) of NNC mice. Scale bar for whole mount H&*E* = 2 mm. Scale bar for H&*E* = 50 μm; images taken at 40x.
(D) IHC images of mouse DMGs in NNC mice incubated with anti-Ki67, anti-HA, anti-Cas9, anti-GFP, or anti-p53 antibody and biotinylated secondary antibody. Scale bar for IHC images = 50 μm; images taken at 40x.
(E) IHC images of non-tumor brain tissue in NNC mice incubated with anti-Ki67, anti-HA, anti-Cas9, anti-GFP, or anti-p53 antibody and biotinylated secondary antibody. Scale bar for IHC images = 50 μm; images taken at 40x.

middle of the pup's head to enter the midline.

Immunohistochemistry

Whole mouse brains were collected upon presentation of humane end points. Brains were fixed in 10 % formalin for 24-72 h before being transferred to 70 % ethanol. For histological analysis, brains were embedded in paraffin wax and cut into sagittal sections for future analysis. Histology was performed by HistoWiz Inc. (histowiz.com). Immunohistochemistry (IHC) was performed on a Bond Rx autostainer (Leica Biosystems) with enzyme treatment (1:1000) using standard protocols. Antibodies used were rabbit monoclonal Cas9 primary antibody (#ab189380), rabbit monoclonal GFP primary antibody (#ab183734), rabbit monoclonal HA-Tag primary antibody (Cell Signaling #3724), rabbit polyclonal Ki67 primary antibody (#ab15580), rabbit polyclonal p53 primary antibody (#NCL-l-P53CM5P), and rabbit polyclonal PTEN primary antibody (#AF847). Bond Polymer Refine Detection (Leica Biosystems) was used according to the manufacturer's protocol. After staining, sections were dehydrated and film coverslipped using a TissueTek-Prisma and Coverslipper (Sakura). Whole slide scanning (40x) was performed on an Aperio AT2 (Leica Biosystems).

Tumor genomic DNA extraction and analysis

To conduct NGS, tumor tissue was identified on H&E sections and then tumor in the formalin-fixed paraffin-embedded (FFPE) block was gently dissected using a scalpel. Genomic DNA was purified using the Qiagen DNeasy Blood & Tissue Kit (#69504). Primers were designed using UCSC Genome Browser [24] and Primer3 [25] (version 4.1.0) to amplify the genetic loci targeted by each of gRNAs via polymerase chain reaction (PCR): *Trp53, Cdkn2a, Atm, Pten* (Supplementary Table 2). Additional primers were designed to examine the representation of the different RCAS vectors after tumor formation by amplifying the sequence containing the spacer gRNA within each construct (Supplementary Table 3). PCR was conducted according to manufacturer's instructions using the DreamTaq Green PCR Master Mix (ThermoFisher #K1081) and purified using the QIAquick PCR Purification Kit (QIAGEN #28104). Sequencing was conducted at GENEWIZ using their Next Generation Sequencing: Amplicon-EZ service (Reference sequences, Supplementary Table 4) and was analyzed in Python (Version 3.13).

Results

CRISPR/Cas9 and RCAS/tv-a drive midline gliomagenesis

We first sought to test if delivery of Cas9 and a gRNA to disrupt *Trp53*, a tumor suppressor that is lost in the majority of DMGs, could stimulate glioma formation in the mouse brain midline. To express Cas9 in neural stem cells in the brain (including the midline), we bred mice of genotype Nestin-tv-a; Nestin-Cre; loxP-Stop-loxP-Cas9-EGFP (NNC). NNC mice were injected with chicken fibroblast cells secreting a retrovirus to express a *Trp53* gRNA (RCAS-Trp53-gRNA-BFP) and a retrovirus to express PDGF-B (RCAS-Cntl-gRNA-PDGFB) and monitored for glioma generation and survival (Fig. 1A; Supplementary Table 5). Median time to tumor formation was 12.6 weeks (Fig. 1B, $P < 0.001$ by log-rank test compared to uninjected mice for which median time to tumor formation was not reached). H&E staining exhibited glioma-like hypercellularity within the tumor and diffuse infiltration of the nearby normal brain (Fig. 1C). Ki67 IHC demonstrated a high proliferation rate of tumor cells characteristic of high grade gliomas (>30 % Ki67 index, Fig. 1D). IHC confirmed the presence of the HA epitope tag on the PDGF-B construct, indicating that the PDGF-B retroviral vectors were successfully integrated into the genome of neural stem cells (Fig. 1D). Cas9 and GFP IHC demonstrated expected Cas9 expression throughout the entirety of the mouse brain (Fig. 1D). Finally, p53 IHC demonstrated a loss of p53 expression within the tumor region (Fig. 1D) as compared to non-tumor regions (Fig. 1E). These results indicate that combined RCAS/tv-a and CRISPR/Cas9 can drive high grade tumor formation in the mouse midline and confirms Cas9-based loss of p53 at the protein level.

Next-generation sequencing confirms CRISPR gene editing in vivo

We next examined somatic alterations in tumors from NNC mice to confirm CRISPR editing of *Trp53*. To do so, we microdissected tumor tissue from FFPE blocks and PCR-amplified the region of mouse *Trp53* targeted by the gRNA (Fig. 2A). NGS showed disruption of p53 in 15.9-86.4 % of DNA across 5 samples, suggesting heterogeneity of tumor and normal cells (Fig. 2B; Supplementary Table 6). Of note, multiple repaired DNA species, characterized by mostly frame shifts resulting from insertions or deletions were isolated (Fig. 2C), suggesting that the tumors originated from multiple cells that received Cas9 and gRNA, rather than a single founder cell. Together, these results confirm on-target CRISPR gene disruption and reveal a multiclonal origin of the mouse midline gliomas.

Endogenous and retroviral Cre delivery can both drive gliomagenesis in the mouse midline

Cre-recombinase is needed to induce Cas9 expression from the Rosa26-loxP-Stop-loxP-Cas9-EGFP allele to enable CRISPR/Cas9-driven midline gliomagenesis. We next examined whether either of two methods to deliver Cre-recombinase could drive gliomagenesis: (i) expression of Cre in neural stem cells throughout the mouse brain using a Nestin-Cre allele in the mouse genome, or (ii) delivery of Cre via a RCAS retrovirus to Nestin-tv-*a*+ neural stem cells specifically in the midline (Fig. 3A). To do so, we examined NNC mice injected with virus-secreting cells transfected with RCAS-Trp53-gRNA-BFP and RCAS-Cntl-gRNA-PDGFB, similarly to the previous experiment. We compared these to mice of genotype Nestin-tv-a, Rosa26-loxP-Stop-loxP-Cas9-EGFP (NC) which were additionally injected with cells transfected with RCAS-Cre. As expected, IHC revealed Cas9 expression in all Nestin+ neural stems cells in both the tumor and normal brain in the NNC mice (Fig. 3B). In the NC approach, Cas9 is only expressed within the tumor cells (Fig. 3C). We observed higher tumor penetrance and decreased time to tumor formation for mice bearing the Nestin-Cre allele in NNC mice, as compared to retroviral delivery of Cre from an RCAS construct (Fig. 3D; Supplementary Table 5). These results show that multiple approaches to

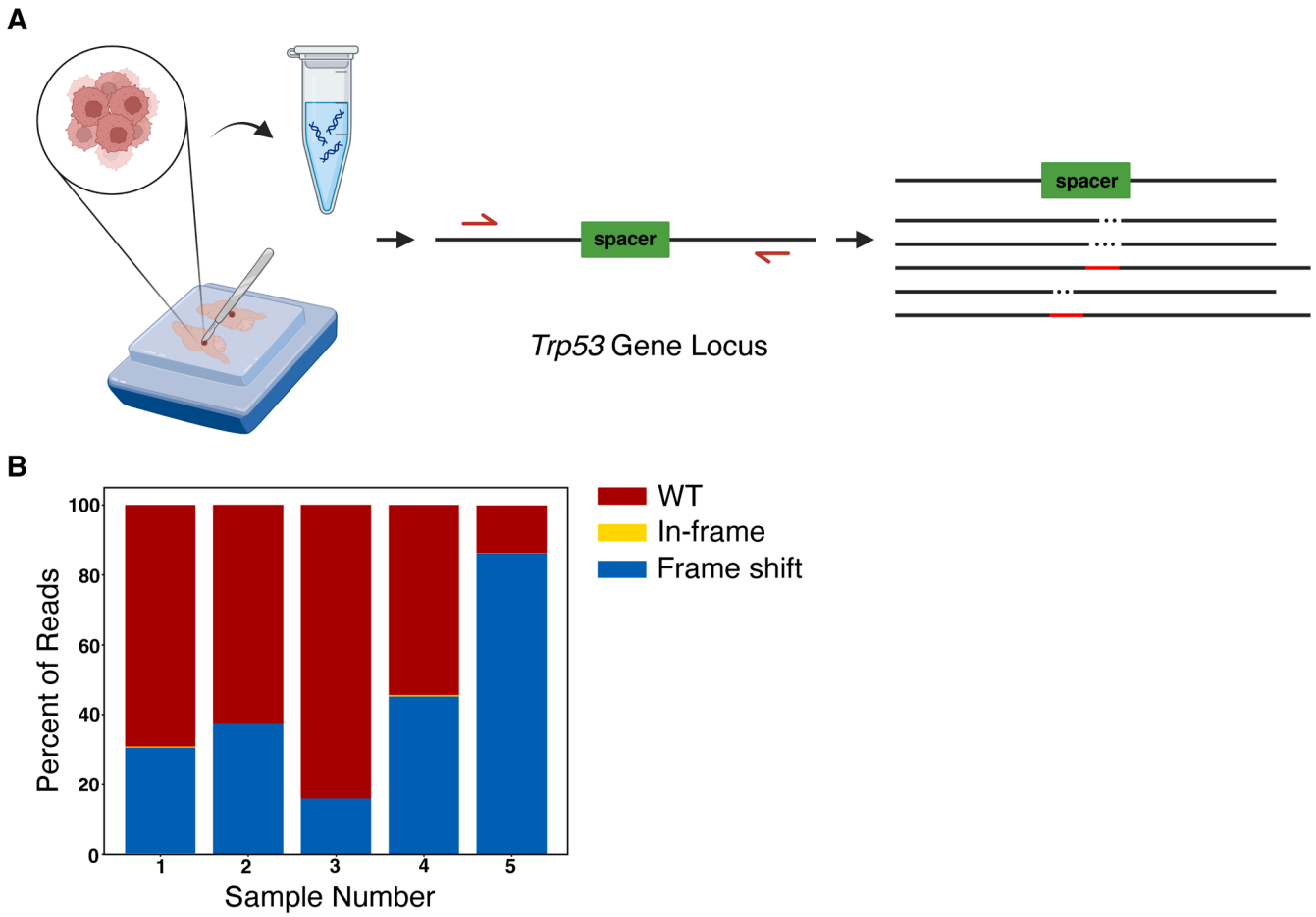

C

Sequencing Reads	Percentage	Type	Indel Length
CCCAAGTGAAGCCCTCCGAGTGTCAGGAGCTCC	78.87	WT	0
CCCAAGTGAAGCCCTCCGAGTTGTCAGGAGCTCC	19.37	Insertion	1
CCCAAGTGAAGCCCTCCGA - - GTCAGGAGCTCC	1.07	Deletion	-2
CCCAAGTGAAGCCCTCCGAG - - - - - - - - GCTCC	0.42	Deletion	-8
CCCAAGTGAA - - - - - - - - - - TGTCAGGAGCTCC	0.19	Deletion	-10
CCCAAGTGAAGCCCTCCGAGTCGTCAGGAGCTCC	0.03	Insertion	1
CCCAAGTGAAG - CCTCCGAGTGTCAGGAGCTCC	0.02	Deletion	-1
CCCAAGTG - AGCCCTCCGAGTGTCAGGAGCTCC	0.02	Deletion	-1
CCCAAGTGAAGCCC - CCGAGTGTCAGGAGCTCC	0.02	Deletion	-1

Fig. 2. NGS of DNA from tumor-bearing mice.
(A) Tumors were microdissected from FFPE mouse brains and genomic DNA purified. PCR amplified the region of *Trp53* targeted by the injected RCAS-Trp53-gRNA-BFP construct. The DNA purified from PCR mixture was sequenced via NGS.
(B) Heterogenous distribution of NGS reads for the *Trp53* gene loci across samples.
(C) NGS sequencing reads for Sample 1.

deliver Cre-recombinase can drive gliomagenesis in the current system.

Cas9-mediated disruption of multiple drivers accelerates midline gliomagenesis

We next examined the feasibility of pooled gRNA experiments in mice with CRISPR/Cas9 machinery. A mini pooled *in vivo* CRISPR experiment was conducted by pooling five different RCAS-gRNA-PDGFB vectors. We selected gRNAs targeting tumor suppressors known to play a role in DMG biology, including *Atm, Cdkn2a, Pten, Trp53* and a non-targeting control (*Cntl*) gRNA (Fig. 4A). Virus-secreting cells were combined in equal proportion and injected into NNC mouse pup

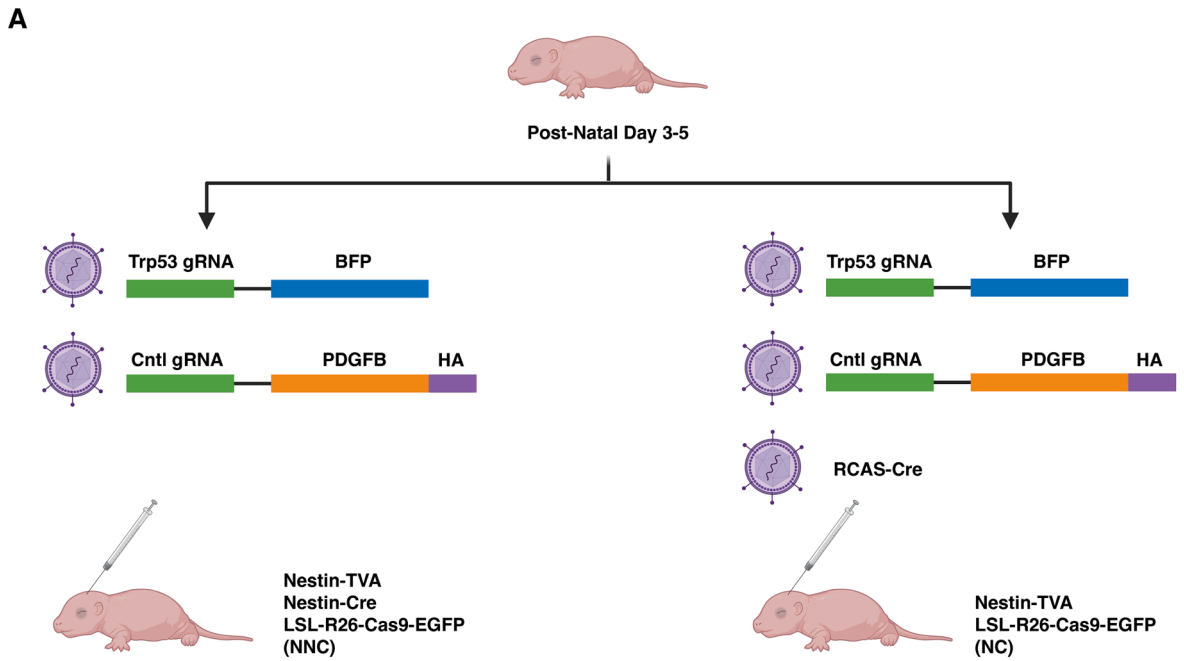

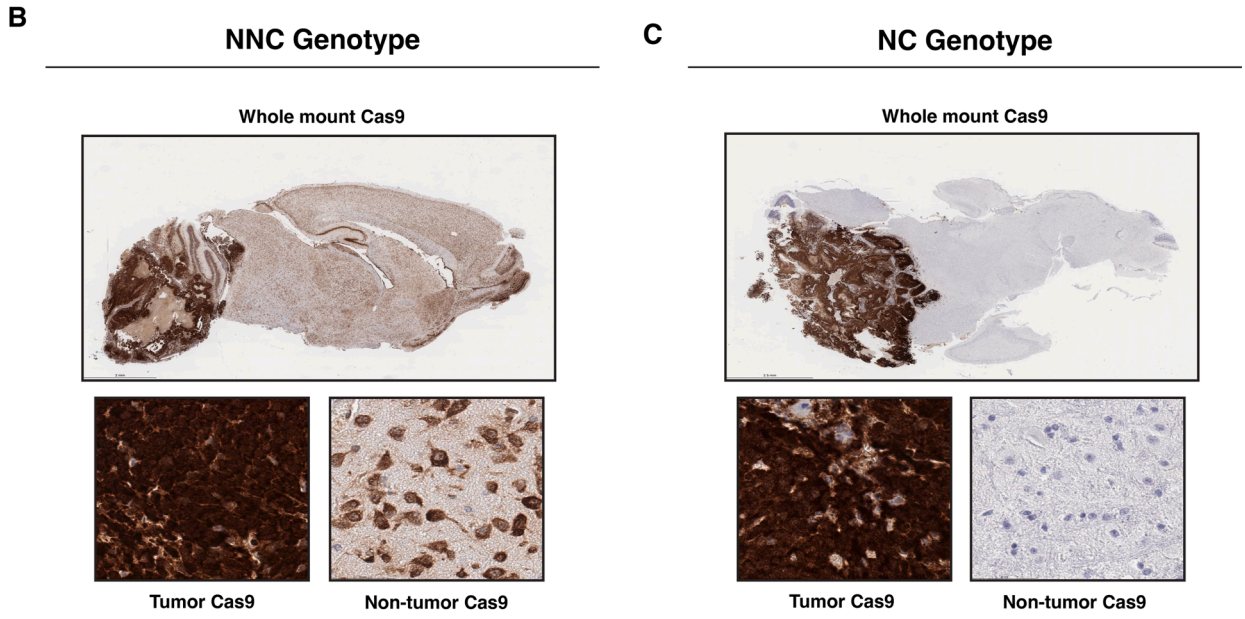

D

	NNC Genotype	NC Genotype
Penetrance	25%	11%
Median Time to Tumor Formation	10.14 weeks	14.40 weeks

Fig. 3. Two approaches to generate tumors containing CRISPR/Cas9 perturbations.
(A) On the left, Cre-recombinase is expressed from an endogenous Nestin-Cre allele in the germline to drive Cas9 expression in all Nestin+ neural stem cells (NNC mice), allowing the use of only 2 viral constructs. On the right, Cre is delivered via a third retroviral construct (NC mice).
(B) Anti-Cas9 IHC for NNC mice brain tissue. Scale bar for whole mount IHC = 2 mm. Scale bar for IHC of tumor and non-tumor tissue = 50 μm; images taken at 40x.
(C) Anti-Cas9 IHC for NC mice brain tissue. Scale bar for whole mount IHC = 2 mm. Scale bar for IHC of tumor and non-tumor tissue = 50 μm; images taken at 40x.
(D) Tumor penetrance and median time to tumor formation for NNC and NC mice.

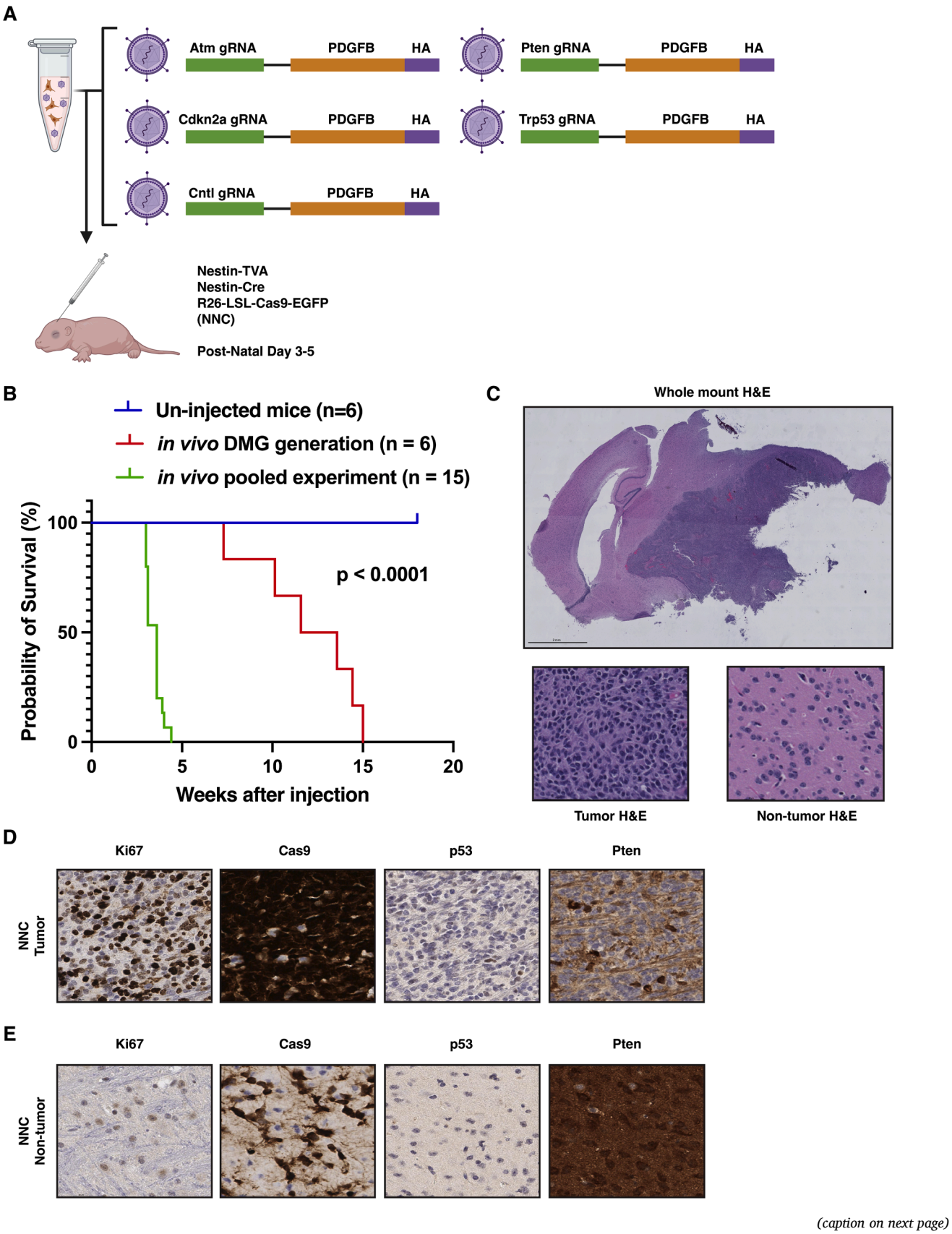

(caption on next page)

Fig. 4. Pooled *in vivo* CRISPR experiment.
(A) Post-natal day 3-5 NNC mice were intracranially injected with virus-secreting DF1 chicken fibroblast cells transfected with RCAS-gRNA-PDGFB plasmids targeting *Atm, Cdkn2a, Pten,* and *Trp53* respectively.
(B) Kaplan-Meier analysis of mice monitored for survival following injection (mice analyzed in Fig. 1 are shown for reference, P-value for log-rank test shown).
(C) Whole mount (top) and H&E slides showing tumor (bottom left) and non-tumor (bottom right) of NNC mice. Scale bar for whole mount H&*E* = 2 mm. Scale bar for H&*E* = 50 μm; images taken at 40x.
(D) IHC images of NNC mouse midline gliomas incubated with anti-Ki67, anti-Cas9, anti-p53, and anti-Pten antibody and biotinylated secondary antibody. Scale bar for IHC images = 50 μm; images taken at 40x.
(E) IHC images of NNC mouse non-tumor brain tissue incubated with anti-Ki67, anti-Cas9, anti-p53, and anti-Pten antibody and biotinylated secondary antibody. Scale bar for IHC images = 50 μm; images taken at 40x.

midlines. Tumors arose with a median time to tumor formation of 3.6 weeks ($P < 0.001$ by log-rank test compared to *Trp53* gRNA alone, Fig. 4B). H&E staining displayed dense cellular formations within the tumor region (Fig. 4C) with high Ki-67 proliferation index (Fig. 4D). IHC confirmed Cas9 expression and loss of p53 and Pten expression at the protein level within the tumors (Fig. 4D) as compared to the non-tumor-bearing brain (Fig. 4E). The results suggest that CRISPR/Cas9 disruption of multiple glioma-associated tumor suppressors can accelerate primary midline gliomagenesis.

Multiplexed gRNAs drive polyclonal tumors and multiple edits in individual cells

To characterize primary mouse tumors derived from injection of multiple gRNAs, we quantified somatic editing at gene loci targeted by each gRNA. PCR amplification of tumor DNA and subsequent NGS was employed for the *Atm, Cdkn2a, Pten*, and *Trp53* genes (Fig. 5A). CRISPR-mediated disruption of all targeted gene loci was observed in all tumors examined. On average across 5 samples, 31.8 %, 41.1 %, 40.7 %, and 34.7 % of the DNA at each gene was disrupted respectively (Fig. 5B; Supplementary Table 7). *Trp53* was the first or second most-disrupted gene in the majority of samples (4/5). All gRNA target sites were associated with multiple indel species (range of 4-26 indel species with >0.2 % representation, mean 12 species), indicating that each gRNA perturbed multiple cells that contributed to the tumor (Supplementary Table 8). However, almost all tumors demonstrated dominant indel species at each site accounting for >50 % of all indel species at that site and/or preferential Cas9 editing events at different sites. The presence of >30 % of DNA containing edits at $n = 4$ sites excludes the possibility that all tumor cells contained only a single edit, indicating that many neoplastic cells must contain two or more CRISPR-induced edits. Thus, multiplexed gRNAs produce polyclonal mouse tumors composed of cells with multiple desired CRISPR edits.

We next hypothesized that gRNA representation could be assessed by quantifying unique barcodes associated with each RCAS-gRNA-PDGFB construct. PCR was used to amplify the unique spacer gRNA site from each construct, and NGS was used to quantify the relative abundance of the different gRNAs (Fig. 5A). Mean representation was 17.3 %, 10.9 %, 20.0 %, 30.9 %, and 20.9 % respectively for the RCAS constructs targeting *Atm, Cdkn2a, Pten, Trp53*, and the non-targeting *Cntl* (Fig. 5C; Supplementary Table 9). The *Trp53* barcode was best-represented among the majority of samples (4/5), in line with the *Trp53* genetic loci sequencing results. A trend for correlation between gene perturbation and the barcode representation was observed (for instance, $R^2 = 0.86$, $P = 0.07$ for Sample 1, Fig. 5D). The results confirm that gRNA representation can be assessed by barcode sequencing. Further, evidence of preferential selection for a specific perturbagen (*Trp53* disruption) suggests that the system can read out tumor evolutionary processes.

Discussion

Here we combine RCAS/tv-a and CRISPR/Cas9 to induce gliomas in the mouse midline, providing a flexible platform for DMG research. The model can be initiated through two alternative methods of delivering Cre-recombinase (either via an exogenous retrovirus or from an endogenous Nestin-Cre allele). We demonstrate feasibility of mini pooled *in vivo* experiments by simultaneously delivering gRNAs targeting multiple tumor suppressor genes relevant to DMG. Genetic characterization indicates that the resultant tumors are polyclonal and driven by multiple driver perturbations. We observed relative selection for *Trp53* disruption, indicating that the platform could be used to identify perturbations that are selected during tumor evolution. These results describe a model of midline glioma that may be useful for future research probing the effects of specific genetic perturbations on tumorigenesis, tumor evolution, tumor-immune interactions, treatment response, and/or resistance mechanisms.

The current study advances previous primary brain tumor modeling work on several levels. The results build on work that combined RCAS/tv-a and CRISPR/Cas9 in adult supratentorial mouse tumors [18]. First, we show that the RCAS/tv-a and CRISPR/Cas9 approach can drive tumorigenesis in the midline which may be relevant to model biological and anatomic aspects of pediatric and/or midline gliomas. Additionally, we characterize genetic composition of tumors induced with multiple (>2) gRNAs. Previous studies tracked retrovirus integration sites to carry out forward genetic screens [26] and used genetic barcoding to explore primary mouse glioma clonal dynamics [27]. Our observation of putative dominant clones defined by specific CRISPR-induced indel species align with previous findings [27]. The current study extends the prior work that examined tumor evolutionary processes in primary mouse gliomas [26] by introducing CRISPR/Cas9 perturbations. These primary mouse brain tumor systems complement a number of glioma allograft and xenograft *in vivo* systems [28–30]. Thus, key advances of the current system are the ability to multiplex perturbations in a primary midline glioma *in vivo* and to read out the perturbations in the resulting tumors.

Combining RCAS/tv-a and CRISPR/Cas9 advances DMG modeling by streamlining experimental work, and by unlocking multiplexed *in vivo* experiments. In terms of streamlining experimental work, the strategy may reduce the resources needed to generate new models and to introduce *in vivo* perturbations. Current methods frequently require breeding of animals to contain multiple complex alleles to inactivate tumor suppressors or genes of interest. These classic approaches often require months to years of mouse breeding and maintenance of multiple complex mouse strains. CRISPR/Cas9-based methods may enable investigators to maintain a single strain (such as the NNC strain) and generate retroviral constructs with different gRNAs whenever new genes must be perturbed. In terms of multiplexed experiments, our mini-pooled gRNA experiments suggest preferential selection for specific perturbagens (*Trp53*; Fig. 5), indicating that *in vivo* screening is feasible. This may enable screens to identify perturbations that affect tumorigenesis, tumor-immune interactions, or response to treatment.

Our study has several limitations. First, we have not directly examined perturbations at the single cell level, precluding a finer understanding of tumor cell clonality and gene editing per-cell. Second, our multiplexed experiments were small ($n = 4$ gRNAs) and it remains unclear how many gRNAs can be practically combined in an experiment. Third, we did not include the *H3f3a* K27M mutation found in DMG in the current system, which may limit the ability to model the unique epigenetic state of DMG. Future work will seek to address these issues and to leverage the system to streamline and multiplex experiments.

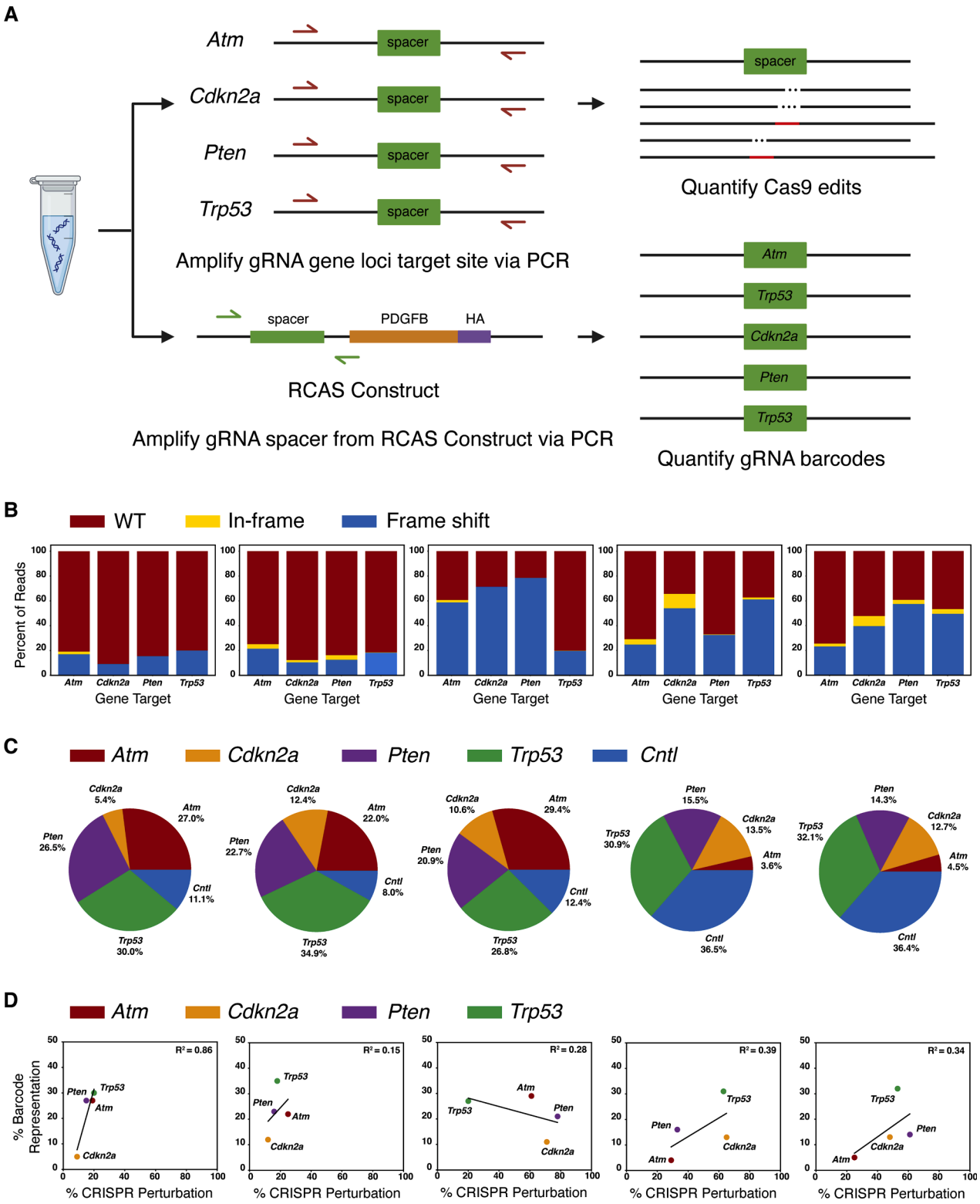

Fig. 5. NGS sequencing for NNC mice receiving multiple pooled gRNAs.
(A) Tumor DNA was microdissected from FFPE blocks and PCR amplified for the *Atm, Cdkn2a, Pten*, and *Trp53* gene loci targeted by their respective synthetic gRNA constructs before NGS sequencing. A similar PCR amplification was done targeting the unique barcode sequence on each of the injected RCAS constructs and NGS sequenced.
(B) Distribution of NGS reads for the *Atm, Cdkn2a, Pten*, and *Trp53* gene loci of five experimental samples.
(C) Barcode representation for the injected RCAS constructs: *Atm, Cdkn2a, Pten, Trp53*, non-targeting *Cntl*.
(D) Relationship between the representation of CRISPR perturbation for a specific gene loci as compared to the representation of the associated gRNA barcode sequence in the mouse DNA.

Conclusion

Here we generated primary mouse gliomas in the midline of the mouse brain using the RCAS/tv-a retrovirus system and the CRISPR/Cas9 gene disruption platform. The system may streamline future experiments, as a gene of interest can now be disrupted by generating a retrovirus construct with a new gRNA for injection into a Cas9-expressing mouse strain. This process is considerably less resource-intensive than breeding new mouse strains that contain perturbations of the gene of interest in their germline. The data suggest that expressing Cre from the mouse germline provides superior tumor penetrance as opposed to injecting an RCAS-Cre virus into the NC strain. Pooled gRNA experiments indicate that multiple gRNAs can be delivered to the same mouse brain tumor, that disruption of multiple tumor suppressor genes may decrease tumor latency, and that the system may be able to read out selection for specific perturbations during tumor evolution. These results establish a system that may accelerate study of tumorigenesis, tumor-immune interactions, and therapeutic approaches for DMG.

CRediT authorship contribution statement

Sophie R. Wu: Conceptualization, Formal analysis, Investigation, Methodology, Project administration, Software, Validation, Visualization, Writing – original draft, Writing – review & editing. **Julianne Sharpe:** Investigation, Writing – original draft. **Joshua Tolliver:** Investigation. **Abigail J. Groth:** Investigation. **Reid Chen:** Investigation. **María E. Guerra García:** Investigation, Resources. **Vennesa Valentine:** Investigation. **Nerissa T. Williams:** Resources. **Sheeba Jacob:** Investigation, Writing – review & editing. **Zachary J. Reitman:** Conceptualization, Funding acquisition, Methodology, Project administration, Supervision, Writing – original draft, Writing – review & editing.

Declaration of competing interest

The authors declare the following financial interests/personal relationships which may be considered as potential competing interests:

Zachary J. Reitman has received royalties for intellectual property related to brain tumor diagnostic tests that is managed by Duke University and has been licensed to Genetron Health, and honoraria from Oakstone Publishing, the NIH, and Eisai Pharmaceuticals. None of these entities played a role in the design or execution of the current study.

Acknowledgements

We thank Charles A. Gersbach, Sharon Gerecht, and David G. Kirsch for advice on this project. Schematics were created with Biorender.com. This research was supported by funds from the Lauren Brescia Memorial Funds, Alex's Lemonade Stand Foundation A Award, ChadTough Defeat DIPG, the Pediatric Brain Tumor Foundation, the St. Baldrick's Foundation, and NIH/NCI K08CA2560456.

Supplementary materials

Supplementary material associated with this article can be found, in the online version, at doi:10.1016/j.neo.2025.101139.

References

[1] V. Di Ruscio, et al., Pediatric diffuse midline gliomas: an unfinished puzzle, Diagnostics 12 (2022) 2064.
[2] E.Y. Akdemir, Y. Odia, M.D. Hall, M.P. Mehta, R. Kotecha, An update on H3K27M-altered diffuse midline glioma: diagnostic and therapeutic challenges in clinical practice, Pract. Radiat. Oncol. 14 (2024) 443–451.
[3] C. Coleman, et al., Interdisciplinary care of children with diffuse midline glioma, Neoplasia 35 (2023) 100851.
[4] D. Hambardzumyan, N.M. Amankulor, K.Y. Helmy, O.J. Becher, E.C. Holland, Modeling adult gliomas using RCAS/t-va technology, Transl. Oncol. 2 (2009) 89–IN6.
[5] S. Rajendran, et al., Single-cell RNA sequencing reveals immunosuppressive myeloid cell diversity during malignant progression in a murine model of glioma, Cell Rep. 42 (2023) 112197.
[6] G. Rao, C.A. Pedone, C.M. Coffin, E.C. Holland, D.W. Fults, c-Myc enhances sonic hedgehog-induced medulloblastoma formation from Nestin-expressing neural progenitors in mice, Neoplasia 5 (2003) 198–204.
[7] N.C. Jenkins, et al., Somatic cell transfer of c-myc and bcl-2 induces large-cell anaplastic medulloblastomas in mice, J. Neurooncol. 126 (2016) 415–424.
[8] Y. Tomita, et al., A novel mouse model of diffuse midline glioma initiated in neonatal oligodendrocyte progenitor cells highlights cell-of-origin dependent effects of H3K27M, Glia 70 (2022) 1681–1698.
[9] C.E. Stewart, et al., The effect of atm loss on radiosensitivity of a primary mouse model of pten-deleted brainstem glioma, Cancers 14 (2022) 4506.
[10] T. Oh, et al., Immunocompetent murine models for the study of glioblastoma immunotherapy, J. Transl. Med. 12 (2014) 107.
[11] R. Wouters, S. Bevers, M. Riva, F. De Smet, A. Coosemans, Immunocompetent mouse models in the search for effective immunotherapy in glioblastoma, Cancers 13 (2020) 19.
[12] B. Olson, Y. Li, Y. Lin, E.T. Liu, A. Patnaik, Mouse models for cancer immunotherapy research, Cancer Discov. 8 (2018) 1358–1365.
[13] R. Zhou, X. Tang, Y. Wang, Emerging strategies to investigate the biology of early cancer, Nat. Rev. Cancer (2024), https://doi.org/10.1038/s41568-024-00754-y.
[14] A. Katti, B.J. Diaz, C.M. Caragine, N.E. Sanjana, L.E. Dow, CRISPR in cancer biology and therapy, Nat. Rev. Cancer 22 (2022) 259–279.
[15] Z. Tothova, et al., Multiplex CRISPR/Cas9-based genome editing in Human hematopoietic stem cells models clonal hematopoiesis and myeloid neoplasia, Cell Stem Cell 21 (2017) 547–555, e8.
[16] S. Annunziato, et al., *In situ* CRISPR-Cas9 base editing for the development of genetically engineered mouse models of breast cancer, EMBO J. 39 (2020) e102169.
[17] H. Kashima, et al., A novel CRISPR/Cas9-mediated mouse model of colon carcinogenesis, Cell Mol. Gastroenterol. Hepatol. 18 (2024) 101390.
[18] B. Oldrini, et al., Somatic genome editing with the RCAS-TVA-CRISPR-Cas9 system for precision tumor modeling, Nat. Commun. 9 (2018) 1466.
[19] R.J. Platt, et al., CRISPR-Cas9 knockin mice for genome editing and cancer modeling, Cell 159 (2014) 440–455.
[20] S.A. Giusti, et al., Behavioral phenotyping of Nestin-Cre mice: implications for genetic mouse models of psychiatric disorders, J. Psychiatr. Res. 55 (2014) 87–95.
[21] E.C. Holland, W.P. Hively, V. Gallo, H.E. Varmus, Modeling mutations in the G_1 arrest pathway in human gliomas: overexpression of *CDK4* but not loss of *INK4a–ARF* induces hyperploidy in cultured mouse astrocytes, Genes Dev. 12 (1998) 3644–3649.
[22] J.G. Doench, et al., Optimized sgRNA design to maximize activity and minimize off-target effects of CRISPR-Cas9, Nat. Biotechnol. 34 (2016) 184–191.
[23] L.B. Weidenhammer, et al., Inducing primary brainstem gliomas in genetically engineered mice using RCAS/TVA retroviruses and Cre/loxP recombination, STAR Protoc. 4 (2023) 102094.
[24] W.J. Kent, BLAT —The BLAST -like alignment tool, Genome Res. 12 (2002) 656–664.
[25] A. Untergasser, et al., Primer3—New capabilities and interfaces, Nucleic. Acids. Res. 40 (2012) e115–e115.
[26] H. Weishaupt, et al., Novel cancer gene discovery using a forward genetic screen in RCAS-PDGFB-driven gliomas, Neuro Oncol. 25 (2023) 97–107.
[27] D. Ceresa, et al., Early clonal extinction in glioblastoma progression revealed by genetic barcoding, Cancer Cell 41 (2023) 1466–1479, e9.
[28] J. Dubrot, et al., In vivo CRISPR screens reveal the landscape of immune evasion pathways across cancer, Nat. Immunol. 23 (2022) 1495–1506.
[29] R.T. Manguso, et al., In vivo CRISPR screening identifies Ptpn2 as a cancer immunotherapy target, Nature 547 (2017) 413–418.
[30] P. Ji, et al., In vivo multidimensional CRISPR screens identify *Lgals2* as an immunotherapy target in triple-negative breast cancer, Sci. Adv. 8 (2022) eabl8247.